Magnetar giant flares and afterglows as relativistic magnetized explosions

Maxim Lyutikov

University of British Columbia, 6224 Agricultural Road, Vancouver, BC, V6T 1Z1, Canada
and
Department of Physics and Astronomy, University of Rochester, Bausch and Lomb Hall, P.O. Box 270171, 600 Wilson Boulevard, Rochester, NY 14627-0171

lyutikov@phas.ubc.ca

Received / Accepted

ABSTRACT

We propose that giant flares on Soft Gamma-Ray Repeaters produce relativistic, strongly magnetized, weakly baryon loaded magnetic clouds, somewhat analogous to solar coronal mass ejection (CME) events. Flares are driven by unwinding of internal non-potential magnetic fields which leads to slow build-up of magnetic energy outside of the neutron star. For large magnetospheric currents, corresponding to a large twist of external magnetic field, magnetosphere becomes dynamically unstable on Alfvén crossing times scale of inner magnetosphere, $t_A \sim R_{NS}/c \sim 30\mu$sec. The dynamic instability leads to formation of dissipative current sheets through development of tearing mode (Lyutikov 2003). Released magnetic energy results in formation of a strongly magnetized, pair-loaded, quasi-spherically expanding flux rope, topologically connected by magnetic field to the neutron star during the prompt flare emission. Expansion reaches large Lorentz factors, $\Gamma \sim 10-20$ at distances $r \sim 1-2\times 10^7$ cm, where lepto-photonic load is lost. Beyond this radius plasma is strongly dominated by magnetic field, though some baryon loading, with $M \ll E/c^2$, by ablated neutron star material may occur. Magnetic stresses of the tied flux rope lead to late collimation of the expansion, on time scales longer than giant flare duration. Relativistic bulk motion of the expanding magnetic cloud, directed at an angle $\theta \sim 135^\circ$ to the line of sight (away from the observer), results in a strongly non-spherical forward shock with observed non-relativistic apparent expansion and bulk motion velocities $\beta_{app} \sim \cot\theta/2 \sim 0.4$ at times of first radio observations approximately one week after the burst. Interaction with a shell of wind-shocked ISM and then with the unshocked ISM leads to deceleration to non-relativistic velocities approximately one month after the flare.

1. Introduction

Magnetar emission (see,*e.g.* , Woods & Thompson 2004, for review) is powered by dissipation of a non-potential (current-carrying) magnetic field (Thompson *et al.* 2002). Dynamo mechanism operating at birth of neutron stars creates a tangled magnetic field inside a neutron star, which is prevented from unwinding by rigidity of the crust. Current-carrying plasma exerts Lorentz force on the crust, which is mostly balanced by lattice strain. For strong enough magnetic fields, Lorentz force may induce a stress that exceeds the critical stress of the lattice. This leads to crustal motion, which should occur along equipotential surfaces: crust will be rotating. Crustal rotation and associated twist of magnetic field lead to expulsion of the electric current from inside of neutron star into magnetosphere. Dissipation of magnetospheric currents is responsible for persistent emission (Thompson *et al.* 2002), while sudden reconfiguration of magnetic field may produce flares (Lyutikov 2003). Giant flare of SGR 1806-20 on December 27 2004 (we will refer to it as "the GF") puts new constraints on the model that we discuss in this paper.

2. Where was energy stored right before the flare? – In the magnetosphere

2.1. Short rise time

GFs are powered by dissipation of magnetic field energy. One of the principal issues is where most of the magnetic energy has been stored prior to the GF: in the magnetosphere or in the neutron star crust. These two possibilities are related to two models of giant flares of the SGRs. First, a giant flare may result from a *sudden* untwisting of the internal magnetic field Thompson & Duncan (1995, 2001), TD95 and TD01 below. In this case, a large and quick (on time scale on a flare) rotational displacement of the crust leads to *increased twisting of magnetospheric magnetic field lines*. Alternatively, *slow* untwisting of the internal magnetic field leads to gradual twisting of magnetospheric field lines, on time scales much longer than GF, until it reaches a dynamical stability threshold due to increasing energy associated with current-carrying magnetic field. Then *sudden relaxation* of the twist outside the star and associated dissipation and magnetic topology change lead to flares, in analogy with Solar flares and Coronal Mass Ejections (CMEs). Note, that even in case of crustal storage of magnetic field energy before the flare (TD95, 2001), dissipation also occurs in the magnetosphere, not in the crust.

The best test of these two alternatives is the time scale for the development of a flare. Since energy involved in the GF requires that a large fraction of the magnetosphere is affected, a typical size of the active region is of the order of the neutron star radius. Sudden

unwinding of the crust should occur either on shear wave or Alfvén wave crossing time of the star $t_{A,NS} \sim R_{NS}/V_{s,NS} \sim R_{NS}/V_{A,,NS} \sim 0.2{-}0.5$ s (TD95), while magnetospheric instability may develop on time scales as short as Alfvén crossing time of the inner magnetosphere, $t_{A,ms} \sim R_{NS}/c \sim 30\mu$s (Lyutikov 2003). Observations of the December 27 GF show very short rise time ~ 0.25 msec (Palmer *et al.* 2005). *Very short rise time of the GF points to magnetospheric origin of GF* (in a sense that right before the flare the energy to be released is stored in the magnetosphere).

2.2. Pre- and Post-burst evolution of persistent emission

XMM-Newton observation of SGR 1806-20 months before the GF shows an increased activity, with persistent flux increasing by a factor of two, spectrum hardening (photon power law index decreased from 2.2 to 1.5) and spindown increasing (Mereghetti *et al.* 2005), all in agreement with the prediction of twisted magnetosphere model (Thompson *et al.* 2002), implying an increasing twist before the GF. In addition, two months after the GF pulsed fraction and the spin-down rate have significantly decreased and the spectrum softened (Rea *et al.* 2005). The same occurred in SGR 1900+14 following the August 27 GF (Woods *et al.* 2001). All of these effects are consistent with increasing of the twist during the time leading to the GF and decreased twist of external magnetic fields after the GF, brought about by reconnection: (i) in the reconnection model the post-flare magnetosphere is expected to have a simpler structure, as the pre-flare network of currents has been largely dissipated; (ii) non-thermality of the spectrum is a measure of the current strength in the bulk of magnetosphere (Thompson *et al.* 2002; Lyutikov & Gavriil 2005) with softer spectra corresponding to a smaller twist; (iii) spin-down rate depends on the amount of current flowing through open field lines and is smaller for a smaller twist. Note, that since open field lines occupy only a small fraction of magnetosphere, spin-down rate probes current in a relatively small region which should, on one hand, correlate with typical current in the magnetosphere on long time scales, but on the other hand may show large deviations on short time scales.

2.3. Ejecta must carry a lot of magnetic field

Magnetospheric storage and release of energy leads to the following consequences. First, it is hard to see how most of the energy released in the magnetosphere can be spent on heating the surface of the neutron star and generating heavy ion-loaded outflows. Secondly, dissipation of magnetic field cannot create magnetic field-free plasma: it is likely to be limited to equipartition fields since at this point induced magnetic field of gyrating relativistic

particles will create magnetic field comparable to the initial field (at temperatures near 500 keV energy in photons will be comparable to energy in electrons). Thus, only approximately half of the magnetic field is expected to be converted to particle and photon energy, not much more. Most of the dissipated energy will be later radiated away and/or spent on pdV work during expansion.

Thus, magnetospheric release of energy, indicated by very short rise time of the GF, decreasing persistent emission and softer post-flare spectrum, leads to the conclusion that expanding plasma must be strongly magnetically dominated. In this paper we examine consequences and consistency of the model based on these premises.

3. Overview of the model

Before discussing various details, let us present a short overview of the model, which qualitatively resembles models of Solar flares with the difference that Sun supports an actively operating dynamo, while in magnetars dynamo operated only during birth of a neutron star. The energy that will be released in a GF is initially (at times long before the flare) stored in electric currents flowing inside neutron star. These currents are generated during birth of the neutron star and are slowly pushed out into magnetosphere, gated by *slow, plastic deformations* of neutron star crust. This creates active magnetospheric regions, in analogy with Solar spots. An active region consists of a sheared arcade of magnetic flux and surrounding non-potential magnetic structures. As currents (and with them magnetic energy and helicity) are pushed outside the neutron star, magnetosphere adjusts slowly to the changing boundary conditions. During this phase magnetic energy is slowly stored in the magnetosphere. As more current is pushed outside, magnetosphere reaches a point of dynamical instability beyond which stable equilibrium cannot be maintained. Crossing the instabilities threshold leads to changing of magnetic configuration on Alfvén crossing time scale, formation of narrow current sheets, and onset of magnetic dissipation (this process is sometimes called magnetic detonation (*e.g.* Cowley and Artun 1997)). This has two consequences. First, a large amount of magnetic energy is converted into kinetic plasma energy and photons. Secondly, dissipation allows to change magnetic topology and leads to formation of an expanding magnetic loop that eventually break away from the star. Initially, after onset of reconnection, kinetic pressure of optically thick pair plasma and magnetic stresses are comparable, so that expansion is quasi-isotropic and reaches relativistic Lorentz factors ≥ 10, determined either by baryon loading or, in case of very small baryon loading, by the amount of residual pairs.

During the prompt phase of the GF, the expanding magnetic *loop remains attached to*

the star, see Fig. 1. Tying of the expanding loop to the star eventually leads to collimation of the explosion into a wide opening angle, of the order of one steradian. After losing the pair load, the expanding cloud is dominated by magnetic field (magnetic cloud) and eventually disconnects form the neutron star, moving relativistically *away* from the observer at an angle $\sim 135^\circ$ degrees. This results in apparent subluminal proper expansion and proper velocity. Eventually, energy of the magnetic cloud is transfered to the strongly anisotropic forward shock which produces the observed afterglow radio emission.

4. Prompt and tail emission of the GF

4.1. Twisting of external magnetic field and GF precursors

The central point of our suggestion is that winding-up of external magnetic field proceeds on long time scale, much longer than GF. The winding can occur on time scale of approximately two months before the GF, indicated by increased activity of the source (Mereghetti *et al.* 2005). Alternatively, onset of fairly rapid plastic deformation of the crust may be related to weak emission events (precursors) that seem to precede GFs. [In case of GF of SGR 1900+14 a precursor was seen ~ 0.4 seconds before the main burst (Feroci et al. 2001) while in case of SGR 1806 a relatively powerful event occurs approximately hundred fourty seconds before the main burst (Palmer *et al.* 2005).] During the quiescent period between the precursor and GF, a patch of a crust is continuously rotated by the Lorentz force, balanced both by elastic and viscous stresses in the crust. These two possibilities are not mutually exclusive: slow evolution on time scale of months may be followed by a relatively fast twisting over hundreds of seconds before the GF.

Consider a crustal plate of size R rotating under the influence of Lorentz force, balanced by viscous stresses at the base of the crust. The dissipated power is (Landau & Lifshitz 1975)

$$L_{visc} \sim \frac{4\sqrt{2}\pi^{7/2}\sqrt{\nu}R^4\rho}{T_{rot}^{5/2}} = 1.3\times 10^{37}\mathrm{ergs}^{-1}\left(\frac{R}{10\mathrm{km}}\right)^4\left(\frac{\rho}{10^{14}\mathrm{gcm}^{-3}}\right)\left(\frac{\Delta\phi}{2\pi}\right)^{5/2} \qquad (1)$$

where $\nu \sim 10^4\left(\frac{\rho}{10^{14}\mathrm{gcm}^{-3}}\right)^{5/4}$ is the viscosity of neutron star (Cutler & Lindblom 1987), ρ is density at the base of the crust, $T_{rot} = 140\left(\frac{\Delta\phi}{2\pi}\right)$ s is the rotation period of the plate, taking into account that instability occurs after rotation of $\Delta\phi$ radians. Total viscously dissipated energy is $E_{vis} \sim L_{visc}T \sim 2\times 10^{39}$ erg. [For SGR 1900+14 with $T_{rot} = 0.4$ sec $L_{visc} \sim 3\times 10^{43} ergs^{-1}$ and $E_{vis} \sim 10^{44}$ erg, but a very short T_{rot} may indicate that twist was near critical before onset of rotation, $\Delta\phi \ll 1$.] Since this energy is released deep in the crust, where thermal diffusion time to the surface is much longer than T_{rot}, most of the

heat is absorbed by the core (*cf.* Lyubarsky *et al.* 2002) and does not show as increased persistent emission between the precursor and the main flare.

During plastic creep, elastic strain is much larger than plastic strain. The difference between the two can be expressed in terms of how much magnetic field exceeds field at the critical strain:

$$\Delta B \sim 2^{9/4}\pi^{3/4}\sqrt{R\rho}\nu^{1/4}T_{rot}^{-3/4} = 2.7\times10^{10}\mathrm{G}\left(\frac{R}{10\mathrm{km}}\right)^{1/2}\left(\frac{\rho}{10^{14}\mathrm{gcm}^{-3}}\right)^{1/2}\left(\frac{\Delta\phi}{2\pi}\right)^{3/4} \quad (2)$$

($\Delta B = 2.2\times10^{12}$ G for SGR 1900+14). Thus, during plastic creep only a small fraction of magnetic energy is dissipated in the crust, most of it is pumped outside of the star.

Note that in case of the Sun, TRACE satellite has detected rotation of sunspots associated with largest (X-class) flares days before the flare (Mewaldt *et al.* 2005). In addition, Solar CMEs also starts before the accompanying X-ray flare: there is a quiet growth period of approximately 30 minutes before formation of the dissipative current sheet (Zirin 1988).

4.2. During the giant flare expansion must be relativistic

Relativistic expansion at the time of the GF follows from the conventional compactness argument. For luminosity $L\sim10^{47}$ erg/s and variability time scale $\sim$ 1msec, optical depth to pair-production is (see also Nakar *et al.* 2005)

$$\tau_{\gamma-\gamma} \sim \frac{L\sigma_T}{4\pi mc^3 R_{NS}} \sim 2\times10^{11} \quad (3)$$

If plasma were to remain non-relativistic, photon diffusion times would be long, inconsistent with short observed variability time scale. This estimate immediately excludes large baryon loading: M must be $\ll E/c^2$. This has always been a standard view of giant flares, (Feroci et al. 2001; Thompson & Duncan 2001). [A possibility that initial γ-ray spike was produced in a relativistic outflow without dynamically important magnetic field and did not contribute significant amount of energy to afterglow is hard to reconcile with magnetospheric origin.]

At early stages dissipation of magnetic field creates an optically dense lepto-photonic plasma emerged in magnetic field with $T\sim(L/4\pi R_{NS}^2\sigma_{ST})^{1/4}\sim300$ keV (see also Nakar *et al.* 2005). Qualitatively, quasi-spherical expansion of a strongly magnetized pair bubble resemble the unmagnetized case, but there are important differences in the asymptotic dynamics, outlined in Appendix A. Initially, plasma expands with bulk Lorentz factor increasing approximately linearly with radius $\Gamma\propto r$, while rest temperature decreases $T\sim1/r$. After reaching $T_\pm\sim20$ keV at $r_\pm\sim1.5\times10^7$ cm (at which point $\Gamma\sim15$), plasma becomes optically thin. Observed emission is thermal with $T_{obs}=\Gamma T_\pm\sim300$ keV.

The main implication of relativistic expansion is that outflow is *not* heavily loaded with baryons. In §6 we will show that this picture is consistent with *observed* non-relativistic expansion velocities of the afterglow.

4.3. Initial millisecond spike is nearly isotropic

If initial spike were strongly anisotropic, with luminosities inside and outside some emission cone different by orders of magnitude, then we would have observed many more tails without initial spikes. Not a single tail without a spike has been seen. Tails are obviously only weakly anisotropic, emitted by a trapped fireball (TD95), while their intensity is well above threshold of detectors.

Since initial γ-ray emission is nearly isotropic, it is unlikely to be produced by a strongly jetted outflow (contrary to Yamazaki *et al.* 2005). It is still feasible that the initial spike is weakly anisotropic, with radiation intensity and Lorentz factors changing by some factor ≤ 2 depending on direction. [Note, that tail emission in all cases was of the same order, while the energies of the initial spikes were vastly different. This fact is, on one hand, consistent with some structured jetted emission of the initial spike, so that all bursts are the same but initial spike is viewed from different angles (Yamazaki *et al.* 2005), but on the other hand it contradicts the fact that afterglow emission in case of the GF was several orders brighter, arguing in favor of larger total energetics. Constant tail emission may be explained as a limiting effect of magnetar magnetic field: above some threshold flare energy, the amount of trapped plasma depends only on the strength of confining poloidal magnetic field and not on the amount of the released twist.]

4.4. Time scales of the GF

There are several time scales in the model: first is the slow initial twist of external magnetic field §4.1. Secondly, there are several time scales associated with the GF itself: (i) sub-millisecond initial rise .25 msec (ii) $\sim$ 5 msec rise to the main peak, (iii) hundreds millisecond total duration of the spike, (iv) tens of seconds tail emission. Finally, there is afterglow time-scale from one week to $\sim$ one month, the latter we identify with non-relativistic transition of the ISM blast wave.

Let us discuss the time scales of the GF itself. Primarily, we associate the shortest time scale observed in the burst $\sim$ 0.25 msec with the Alfvén crossing time of the inner magnetosphere. It reflects the dynamical evolution of the magnetosphere after it has

crossed stability threshold. Thus, the very first photons are emitted while plasma is still not expanding relativistically.

Secondly, since emission requires dissipation of energy, dissipative time scales become important as well. In magnetar magnetospheres development of dissipative tearing instability occurs on time scale intermediate between Alfvén times scale and resistive time scale: $t_{tearing} \sim \sqrt{\eta c/R_{NS}}$ where η is plasma resistivity. If resistivity is related to plasma skin depth, $\eta \sim c^2/\omega_p$, where ω_p is plasma frequency, the growth rate of tearing mode is ~ 10 msec for a current sheet of width $\sim R_{NS}$ (Lyutikov 2003). Intermediate time scale ~ 5 msec observed in the GF may be related to development of tearing mode in the current sheets formed during onset of dynamical instability.

We associate the overall duration of the spike ~ 100 msec with the dynamical time of the expanding magnetic cloud $\sim 2\Gamma^2 c/R_{NS} \sim 25$msec for $\Gamma \sim 20$. This is the minimum time it takes for expanding strongly magnetized bubble to come into causal contact with itself. One expects that on this time scale magnetic cloud re-adjusts its internal structure and relaxes to a minimal energy state. This relaxation occurs, *e.g.* , through reconnection, which in relativistic case may proceed with the inflow velocity reaching the velocity of light (Lyutikov & Uzdensky 2003).

Finally, typical time scale for the evolution of the tail of the GF, tens of seconds, is well described by radiation leaking from a plasma trapped on closed magnetic field lines, TD95.

4.5. Quasi-thermal spectrum of the initial spike.

Thermal spectrum results from radiation escaping from a (strongly magnetized) fireball that becomes optically transparent. Observer temperature of hundreds of keV corresponds to rest frame temperature of ~ 20 keV, when plasma becomes optically thin to pair production, boosted by Lorentz factor ~ 10 (Goodman (1986); Paczynski (1986), see also Nakar *et al.* (2005)).

4.6. Mass loading and terminal Lorentz factor

In appendix A we consider dynamics of a hot, strongly magnetized expanding flow carrying toroidal magnetic field. Flow is accelerated by magnetic and pressure forces, while both matter inertia and magnetic field energy density provide effective loading of the flow. In addition, in case of a large scale magnetic field considered here, there is extra conserved quantity: magnetic flux. This plays an important role in the overall dynamics of the flow

(*cf.* Kennel & Coroniti 1984).

If source luminosity is L, mass loss rate is $\dot{M}_0$ and EMF is $\mathcal{E}$ (these are conserved quantities), then the terminal Lorentz factor and terminal magnetization parameter σ_∞ are

$$\Gamma_\infty = \frac{L}{\dot{M}_0(1+\sigma_\infty)},, \quad \sigma_\infty = \frac{\mathcal{E}^2}{\Gamma_\infty \beta_\infty \dot{M}_0}. \tag{4}$$

Which, formally, expresses the fact that magnetic field provides additional effective loading (factor $1+\sigma_\infty$), but the amount of loading depends non-trivially on parameters of the flow. In the strongly relativistic limit, outflow typically reaches Alfvén velocity (in fact fast magnetosonic), at which point Lorentz factor is related to the terminal magnetization parameter as (Michel 1971; Goldreich & Julian 1969)

$$\Gamma_\infty = \sqrt{\sigma_\infty}, \tag{5}$$

To estimate the maximum possible Lorentz factor, we note that the minimum mass loading is determined by residual left-over pairs, determined by equating annihilation and expansion rates (Goodman 1986; Paczynski 1986; Nakar *et al.* 2005)

$$M_{min} = m_e N_\pm = \frac{4\pi R_0 c t T_0^3 m_e}{\sigma_T T_\pm^3} = 2\times 10^{17}\mathrm{g} \tag{6}$$

If most energy is in magnetic form, this corresponds to $\sigma_{max} = E/M_{min}c^2 = 4.5\times 10^7$. The corresponding maximum Lorentz factor is $\Gamma_{max} = \sqrt{\sigma_{max}} = 6.7\times 10^3$. Lower limit on Γ comes from the observed thermal temperature of the initial spike:

$$\Gamma_{min} \sim \frac{T_{obs}}{T_\pm} \sim 10-20 \tag{7}$$

Thus, the flow must be only weakly polluted by baryons. This picture is in full agreement with TD01. In what follows we adopt a minimum value of $\Gamma = 10$ for numerical estimates. Then, estimating $E \sim L t_s$ and $M \sim \dot{M} t_s$ and using Eq. (5), Eq. (5) gives

$$M \sim \frac{E}{\Gamma \sigma c^2} = \frac{E}{\Gamma^3 c^2} \sim 10^{22}\mathrm{g} \tag{8}$$

This is the upper limit on amount of mass ejected during the GF.

4.7. Plasma physics issues

The proposed model of the GF builds on the models of Solar CME and, similarly, has a number of problematic plasma physics issues, (see, *e.g.* Priest & Forbes 2002, for

review) One is what is known as Aly-Sturrock paradox (Aly 1984; Sturrock 1991): opening of field lines, which is necessary to generate an outflow, requires an increase in the magnetic energy in the system, while the storage model of CMEs requires magnetic energy to decrease during formation of magnetic cloud. There is a number of ways Aly-Sturrock paradox can be circumvented, most important being magnetic reconnection which can change topology of the field line.

Another problem is that injection of current occurs on a finite amount of magnetic flux so that in order to expand the newly formed magnetic cloud has to break through overlying closed dipolar field lines. This is achieved by reconnection at the null point at the leading edge of the magnetic cloud, *cf.* "magnetic breakout" model of Antiochos *et al.* (1999). Reconnection transfers unshared magnetic flux associated with overlying dipolar field to neighboring flux tubes, allowing the sheared filament to expand and erupt outward. The rate of reconnecting adjusts so that radial (as seen from the star) propagation velocity is the Alfvén velocity, which in this case is nearly the velocity of light.

5. Radio afterglow: qualitative description

5.1. Expansion in SGR wind

As magnetic cloud expands, it becomes transparent at $r_{\pm}$ and its pair density falls by many orders of magnitude. At this point magnetic cloud becomes strongly magnetically dominated. Initially magnetic cloud is topologically connected to the star, but eventually reconnection should happen at the footpoints of the magnetic field lines, disconnecting the magnetic cloud from the star. At this point magnetic cloud d starts to expand into preexisting SGR wind. It is expected that SGR wind is strongly relativistic, with Lorentz factors $\gg 10-20$. Thus, for intermediate baryon loading (such that magnetic cloud expands with $\Gamma \sim 10-20$) magnetic cloud never overtakes the wind, so that expansion occurs as if in vacuum. Most of the magnetic energy is concentrated in a shell close to the bubble surface with thickness of the order of $ct_s \sim 10^9$ cm, where $t_s \sim 100$ msec is flare duration.

5.2. Apparent constant non-relativistic expansion velocity is due to relativistic strongly anisotropic expansion.

Observations of constant expansion velocity from two to five weeks after the burst have been interpreted as evidence in favor of large baryon loading, and, as a consequence, weak relativistic initial expansion velocities (Granot *et al.* 2005). A we argued above, this cannot

be the case due to compactness constraints: flow must be relativistic with small baryon loading.

Apparent non-relativistic expansion velocity can be due to relativistic anisotropic expansion with little emission within the cone $1/\Gamma$ to the line of sight. If emitting material is moving relativistically at an angle $\theta \gg 1/\Gamma$, then apparent expanding velocity is $\beta_{app} = \beta \sin\theta/(1-\beta\cos\theta) \approx \beta \cot\theta/2$. To reproduce observed $\beta_{app} \sim 0.3-0.4$, it required that outflow is directed away from the observer at an angle $\sim 135^\circ$.

We have arrived at a seeming contradictory picture: initially, during the 0.2 sec spike of the GF, expansion should be nearly isotropic, while at later times, ≥ 1 week expansion is strongly anisotropic. Thus, magnetic cloud should become strongly anisotropic between 0.2 seconds and 7 days. It is unlikely that anisotropy is achieved by internal magnetic stresses of the freely expanding magnetic cloud: in relativistic case self-collimation is strongly suppressed (*e.g.* Bogovalov 2001). Similarly, as we argue in §5.3, collimating effects of the dipolar magnetic field cannot account for strong anisotropy given the nearly spherically symmetric initial explosion. We propose that expanding magnetic cloud becomes strongly anisotropic due to fact that magnetic fields of the cloud remain attached to the neutron star during most of the prompt phase. Thus, at this times the magnetic topology of the expanding plasma is that of a flux rope, see Fig. 1.

5.3. Spheromac or flux rope?

Last decade two models were proposed for the structure of interplanetary magnetic clouds ejected from the Sun: a magnetic flux rope and spheromac. The principal difference between the two is that in case of spheromac, magnetic cloud disconnects from the magnetic field of the Sun at early stages of ejection and becomes quasi-spherical (*e.g.* Gibson & Low 1998), while flux rope remains attached to the Sun for a very long time (even at the orbit of the Earth). The two models lead to very different dynamics of the magnetic clouds. Presently, spheromac model seems to be inconsistent with data (*e.g.* Farrugia *et al.* 1995), while magnetic flux rope model explains well the internal magnetic structure ejected into interplanetary space (Marubashi 2000).

In case of the GF, spheromac model seems to be inconsistent with data for the following reason. As we argued above, the initial explosion should be quasi-isotropic, while at later times it should become strongly anisotropic and one-sided. It unlikely that relativistic, strongly anisotropic explosions are produced due to collimating effects of internal magnetic field of the expanding blob which is disconnected from the star: for relativistic expansion

collimation by internal magnetic field is kinematically suppressed (*e.g.* Bogovalov 2001), and in any case cannot produce one-sided explosion. Spheromac also cannot be efficiently collimated by external dipolar magnetic field, since inside spheromac internal kinetic and magnetic pressures scale as $\propto B_{sph}^2 \sim r^{-4}$ (B_{sph} is a typical magnetic field inside spheromac), while $B_{dipolar}^2 \sim r^{-6}$. Thus, if the plasma to be ejected disconnects from the stellar magnetic field early on, one may expect only weak collimation and, as a result, weak relativistic bulk motion. Since the overall expansion should be strongly relativistic, as we argued in §4.2, observed emission will be dominated by parts of the shock moving towards the observer, with somewhat smaller Lorentz factor than average, but having large apparent velocity. To illustrate the point, in Fig 2 we plot Doppler factor $\delta = 1/(\Gamma(1 - \beta\cos\theta)$ and apparent transverse velocity for a relativistic shock expanding with Lorentz factor $\Gamma = 3$ and moving at $\theta_{ob} = 135^\circ$ with bulk Lorentz factor $\Gamma_{bulk} = 2$ as a function of the angle θ between the explosion direction and emission point in the rest frame of the explosion and emission points located in the plane containing direction of bulk motion and line of sight. Points on the shell with highest Doppler boosting have large apparent transverse velocities, in contradiction with observations.

On the other hand, expanding magnetic cloud confined by a flux rope (with $B_{rope}^2 \sim\sim r^{-4}$) may in principal provide collimation (this would correspond to only regions near $\theta_{ob} \leq \pi$ in Fig. 2 contributing to observed emission). Details of this late collimation need to be investigated numerically. From observational point of view, at late times expansion should be confined to a fairly broad angle, of the order of π radians, and not to thin, GRB-like jet.

6. Basic afterglow parameters

6.1. Geometry

For numerical estimates we chose $\theta_{ob} = 3\pi/4 = 135^\circ$. Then apparent velocity $\beta_{app} \sim \beta cot\theta/2 = 0.41\beta$, Doppler factor $\delta \sim 1/(2\Gamma\sin^2\theta/2) = 0.58/\Gamma$ and observer time is given by $T = 2r\sin^2\theta/2/(\beta c) = 1.70r/(\beta c)$. We assume a strongly magnetized flow with total isotropic energy $E_{ej} \sim 10^{46}$ erg which reaches terminal Lorentz factor $\Gamma = 10$, and is collimated into angle $d\Omega/(4\pi) \sim .1$ (so that "typical opening angle is $\sim 36^\circ$). We also normalize surrounding density to $n = 1$ cm^3.

6.2. Typical radii and time scales

Before the explosion, the magnetar is surrounded by a nearly empty bubble blown by the magnetar wind with a typical size

$$r_s \sim \left(\frac{L_w}{4\pi n m_p c V_{NS}^2}\right)^{1/2} \sim 1.2\times 10^{16}\mathrm{cm}\,\left(\frac{n}{1\mathrm{cm}^{-3}}\right)^{-1/2}\,\left(\frac{V_{NS}}{100\mathrm{kms}^{-1}}\right)^{-1} \tag{9}$$

where $L_w \sim 10^{34}$ erg/s is average spindown luminosity of SGR 1806 and V_{NS} is velocity of the neutron star. Since magnetar wind is expected to have Lorentz factor $\Gamma_w \gg 10$, until r_s magnetic cloud expands freely, without slowing down. Note, that r_s is the minimum distance from the neutron star to the shell, depending on the relative orientation of the neutron star velocity and direction of explosion the time when magnetic cloud overcomes the shell can be larger by factor of ~ 2.

Were it to expand in a constant density medium, the flow would starts to decelerate at

$$r_{dec} \sim \left(\frac{3E_{ej}}{d\Omega n m_p c^2 \Gamma_0^2}\right)^{1/3} \sim 5.4\times 10^{15}\mathrm{cm}\left(\frac{E}{10^{46}\mathrm{ergs}^{-1}}\right)^{1/3}\,\left(\frac{n}{1\mathrm{cm}^{-3}}\right)^{-1/3}\,\left(\frac{\Gamma_0}{10}\right)^{-2/3} \tag{10}$$

Since $r_{dec} < r_s$, magnetic cloud starts interacting with the a shell of shocked ISM plasma at $r \sim r_s$. In observer time this occurs at

$$T \sim 1.7\frac{r_s}{c} = 8.2\mathrm{days} \tag{11}$$

Since the amount of the mass contained in a shell of shocked ISM plasma is $\sim n m_p r_s^3$, after encountering the shell Lorentz factor of the magnetic cloud falls down to

$$\Gamma \sim \left(\frac{3E}{d\Omega n m_p c^2 r_s^3}\right)^{1/2} = 2.8\left(\frac{E}{10^{46}\mathrm{ergs}^{-1}}\right)^{1/2}\,\left(\frac{V_{NS}}{100\mathrm{kms}^{-1}}\right)^{3/2}\,\left(\frac{n}{1\mathrm{cm}^{-3}}\right)^{1/4}\,\left(\frac{d\Omega}{0.1\times 4\pi}\right)^{-1/2} \tag{12}$$

Doppler beaming factor at this point is $\delta = 0.2$.

Transition to the non-relativistic expansion occurs at

$$r_{nr} \sim \left(\frac{3E_{ej}}{d\Omega n m_p c^2}\right)^{1/3} \sim 1.7\times 10^{16}\mathrm{cm} \tag{13}$$

corresponding to the observer time

$$T_{nr} = 16.5\mathrm{days} \tag{14}$$

T_{nr} is an estimate of time when the velocity of the blast wave starts to deviate considerably from c. It typically takes two times longer for the velocity to fall below 0.5 c, and for the Doppler factor to become within 15% of unity. One expects to see a peak of emission at the moment when Doppler de-boosting becomes insignificant, approximately at $\sim 2T_{nr} \sim 33$ days.

6.3. Total energy

Form the standard equipartition argument (Pacholczyk 1969), and taking into account Lorentz transformation of flux, $\propto \delta^{3-\alpha}$, and frequency, $\propto \delta$, the minimal energy of relativistic electrons plus magnetic field is

$$E_{min} = 8 \times 10^{44} \mathrm{erg} \left(\frac{\theta}{65''}\right)^{9/7} d_{15}^{17/7} \left(\frac{F_\nu}{50\mathrm{mJy}}\right)^{4/7} \left(\frac{\nu}{8.5\mathrm{GHz}}\right)^{2/7} \left(\frac{\delta}{0.2}\right)^{-2+4\alpha/7} \quad (15)$$

where $\alpha \sim 0.5$ is the spectral index. This estimate is by a factor $\delta^{-2+4\alpha/7} \sim 15$ larger than the one based on assumption of non-relativistic expansion. Corresponding magnetic field (in laboratory frame) is

$$B_{min} = 0.1\,\mathrm{G} \left(\frac{\theta}{65''}\right)^{-6/7} d_{15}^{-2/7} \left(\frac{F_\nu}{50\mathrm{mJy}}\right)^{2/7} \left(\frac{\nu}{8.5\mathrm{GHz}}\right)^{1/7} \left(\frac{\delta}{0.2}\right)^{-1-2\alpha/7}, \quad (16)$$

which is larger by a factor $\delta^{-1-2\alpha/7} \sim 6$ than the one based on assumption of non-relativistic expansion. Note, that minimal energy argument address only energy in magnetic field and relativistic electrons. It is expected that most energy of the forward shock resides in protons, so that the total energy in the outflow may be order(s) of magnitude larger than (15), bringing it in line with the total energy released in γ-rays.

7. Discussion

In this paper we outlined a model of magnetar GF based on the analogy with Solar Coronal Mass Ejections. Very short rise time scales of the GF indicate that GF flare is driven by dissipation of energy stored in the magnetosphere right before the burst (as suggested by (Lyutikov 2003)) and not in the crust of the neutron star (as proposed by TD95). Initially, the explosion is loaded with pairs and is quasi-isotropic. Magnetic field topology of expanding plasma resemble flux rope model of CMEs, which leads to late time collimation and anisotropic expansion. Expanding magnetic cloud is strongly dominated by magnetic field, weakly baryon loaded, with $M \ll E/c^2$, and strongly relativistic. Weeks after the flare, magnetic cloud still expands relativistically, strongly anisotropically and is moving away from the observer, resulting in apparent expansion velocity $\beta_{app} \sim 0.4$. At approximately 33 days, corresponding to a bump in the light curve, expansion velocity falls below $c/2$. The main prediction of the model is that we may see a medium-energy flare with a very bright radio afterglow, when the explosion will be beamed towards the Earth. Statistically, it should take approximately $\sim 1/d\Omega \sim 10$ GFs.

Magnetospheric dissipation following plastic deformation of the crust is also consistent with suggestion of Jones (2003) that that neutron-star matter cannot exhibit brittle fracture and should instead experience only plastic deformations. On the other hand, complexity of earthquakes, especially so called deep focus earthquakes occurring at high pressures, indicates that Jones (2003) argument is not the end of the story. For example, crust response may depend on value of a strain, being plastic at low strains and brittle at high strains (Frohlich 1989).

Can crustal fractures model be consistent with above arguments? One possible way is to invoke small scale, ~ 100 meters, initial crustal deformation (so that the rise time of the GF is short enough), which triggers larger scale deformations in an avalanche-type process (TD95, TD01). In addition, relatively bright and long-lived afterglow following August 27 flare is well fitted by the deep crustal heating model (Lyubarsky *et al.* 2002). The crustal fracture model also has a better chance of explaining post-flare activity (August 27 and March 5th flares followed by a burst-active period) in analogy with earthquake aftershocks.

One possible way to distinguish the models is that reconnection-type events may be accompanied by coherent radio emission resembling solar type-III radio bursts Lyutikov (2002). The radio emission should have correlated pulse profiles with X-rays, narrow-band-type radio spectrum with $\Delta\nu \leq \nu$ with the typical frequency $\nu \geq 1$ GHz, and a drifting central frequency. This requires catching a burst in simultaneous radio and X-ray observations.

We would like to thank Roger Blandford, Yuri Lyubarky and Christofer Thompson for numerous discussions.

REFERENCES

Aly, J. J., 1984, ApJ, 283, 349

Antiochos, S. K. and DeVore, C. R. and Klimchuk, J. A. , 1999, ApJ, 510, 485

Bogovalov, S., 2001, A&A, 371, 1155

Cowley, S. C. and Artun, M., 1997, Phys. Rep., 283, 185

Cutler, C. and Lindblom, L., 1987, ApJ, 314, 234

Gibson, S. E. and Low, B. C., 1998, ApJ, 493, 460

Goldreich, P. & Julian, W. H., 1969, ApJ, 157, 869

Goodman, J. 1986, ApJ, 308, L47

Granot, J. *et al.* , 2005, astro-ph/0503251

Farrugia, C. J. and Osherovich, V. A. and Burlaga, L. F. , 1995, J. Geophys. Res., 100, 12293

Feroci, M., Hurley, K., Duncan, R.C., & Thompson, C., ApJ, 549, 1021

Frohlich, C., 1989, Annual Review of Earth and Planetary Sciences, 17, 227

Israel, G. L., 2005, ApJ, 628, 53

Jones, P. B., 2003, ApJ, 595, 342

Kennel, C. F. & Coroniti, F. V. 1984, ApJ, 283, 710

Landau, L. D. & Lifshitz, E. M. 1975, Course of Theoretical Physics, Vol. 4, Fluid mechanics, 4th edn. (Oxford: Butterworth-Heinemann)

Lyubarsky, Y. and Eichler, D. and Thompson, C., 2002, ApJ, 580, 69

2002, ApJ, 580, 65

Lyutikov, M., 2003, MNRAS, 346, 540

Lyutikov, M., Uzdensky D., 2003, ApJ, 589, 893

Lyutikov, M., Gavriil, F., 2005, submitted to MNRAS, astro-ph/0507557

Marubashi, K., 2000, Advances in Space Research, 26, 55

Mewaldt, R. A. *et al.* 2005, American Geophysical Union, Fall Meeting 2005

Michel F.C. 1971, Comments Ap. Space Phys. 3, 80

Nakar, E. and Piran, T. and Sari, R., 2005, astro-ph/0502052

Pacholczyk, A. G. Radio Astrophysics, W. H. Freeman & Co., San Francisco, 1969.

Paczynski, B. 1986, ApJ, 308, L43

Palmer, D. M. *et al.* , 2005, Nature, 434, 1107

Priest, E. R. and Forbes, T. G., 2002, A&A Rev., 10, 313

Rea, N. and Tiengo, A. and Mereghetti, S. and Israel, G. L. and Zane, S. and Turolla, R. and Stella, L., 2005, ApJ, 627, 133

Schwartz, S. J. *et al.* , 2005, ApJ, 627, 129

Sturrock, P. A., 1991, ApJ,380, 655

Tiengo, A. and Esposito, P. and Mereghetti, S. and Rea, N. and Stella, L. and Israel, G. L. and Turolla, R. and Zane, S. , 2005, astro-ph/0508074

Thompson, C. & Duncan, R.C. 1995, MNRAS, 275, 255 (TD95)

Thompson, C. & Duncan, R.C. 2001, ApJ, 561, 980 (TD01)

Thompson, C., Lyutikov, M., Kulkarni, S. R., 2002, ApJ, 574, 332

Mereghetti, S. *et al.* , 2005, ApJ, 628, 938

Woods, P. M. and Kouveliotou, C. and Göğüş, E. and Finger, M. H. and Swank, J. and Smith, D. A. and Hurley, K. and Thompson, C., 2001, ApJ, 552, 748

Woods, P. M. and Thompson, C., 2004, astro-ph/0406133

Zirin, H., 1988, "Astrophysics of the sun", Cambridge Univ. Press, New York

Yamazaki, R. and Ioka, K. and Takahara, F. and Shibazaki, N. , 2005, PASJ, 57, 11

A. Dynamics of magnetized pair-loaded flows

In this section we consider dynamics of a hot relativistic, spherically symmetric, stationary outflow carrying toroidal magnetic field. Since the energy release during GF lasts ~ 0.1 s, on small time scales and for radii $\leq 10^9$ cm flow may be considered stationary. In addition, internal energy density in the expanding magnetic cloud scales slower with the radius, $\propto r^{-4}$, than energy density of the dipolar field $\propto r^{-6}$, so that dynamical effects of dipolar magnetic field quickly become negligible. At this stage expansion is quasi-isotropic, as discussed in §4.3. Rotation and dynamical effects of the poloidal magnetic field are neglected.

The dynamics of such a warm magnetized wind is controlled by three parameters: energy L, mass flux $\dot{M}$ and the electro-motive force $\mathcal{E}$ produced by the expanding magnetic cloud.

This preprint was prepared with the AAS LaTeX macros v5.2.

Total energy flux may be divided in two forms: mechanical L_M and electromagnetic L_{EM} luminosities.

$$L = L_M + L_{EM} \tag{A1}$$

We wish to understand how the parameters of a fully relativistic flow (velocity β, pressure p, magnetization σ) evolve for an arbitrary ratio of both L_{EM}/L_M and p/ρ (ρ is the rest-frame mass density).

The asymptotic evolution of the flow is determined by conserved quantities which may be chosen as the total luminosity L, the mass flux $\dot{M}$ and the EMF $\mathcal{E}$. Thus, the central source works both as thruster and as a dynamo.

The formal treatment of the problem starts with the set of relativistic MHD equations which can be written in terms of conservation laws. In coordinate form and assuming a stationary, radial, spherically symmetric outflow with toroidal magnetic field, relativistic MHD equations give

$$\frac{1}{r^2}\partial_r \left[r^2(w+b^2)\beta\Gamma^2\right] = 0 \tag{A2}$$

$$\frac{1}{r^2}\partial_r \left[r^2\left((w+b^2)\beta^2\Gamma^2 + (p+b^2/2)\right)\right] - \frac{2p}{r} = 0 \tag{A3}$$

$$\frac{1}{r}\partial_r \left[rb\beta\Gamma\right] = 0 \tag{A4}$$

$$\frac{1}{r^2}\partial_r \left[r^2\rho\beta\Gamma\right] = 0 \tag{A5}$$

The above relations can be simplified by defining

$$L = 4\pi r^2 \beta\,\Gamma^2 \left(b^2 + \frac{\Gamma_a}{\Gamma_a - 1}\,p + \rho\right), \quad \dot{M} = 4\pi r^2 \beta\,\Gamma\,\rho, \quad \mathcal{E} = 2\sqrt{\pi} r\,\beta\,\Gamma\,b \tag{A6}$$

where we assume that fluid is polytropic with adiabatic index Γ_a: $w = \rho + \frac{\Gamma_a}{\Gamma_a - 1}p$, $\mathcal{E}$ is the electromotive force.

It is convenient to introduce two other parameters: the magnetization parameter σ as the ratio of the rest-frame magnetic and particle energy-density and a fast magnetosonic wave phase velocity β_f

$$\sigma = \frac{b^2}{w} = \frac{\mathcal{E}^2}{L\beta - \mathcal{E}^2}, \quad \beta_f^2 = \frac{\sigma}{1+\sigma} + \frac{\Gamma_a p}{(1+\sigma)w} = (\Gamma_a - 1)\left(1 - \frac{\Gamma\dot{M}}{L}\right) + (2 - \Gamma_a)\frac{\mathcal{E}^2}{L\beta} \tag{A7}$$

Using the three conserved quantities L, $\dot{M}$ and $\mathcal{E}$ the evolution equation becomes

$$\frac{1}{2\beta^2\Gamma}\partial_r\Gamma = \frac{(\Gamma_a - 1)\left(\beta L - \beta\Gamma\dot{M} - \mathcal{E}^2\right)}{r\,\left(\beta L(\beta^2 + 1 - \Gamma_a) + (\Gamma_a - 1)\beta\Gamma\dot{M} - (2 - \Gamma_a)\mathcal{E}^2\right)} \tag{A8}$$

Eliminating $\mathcal{E}$ in favor of Γ_f we get a particularly transparent form for the evolution of Lorentz factor

$$\frac{\left(\Gamma^2 - {\Gamma_f}^2\right)}{\beta^2\Gamma^3}\partial_r\Gamma = \frac{2p\Gamma_a}{(w - \Gamma_a p)r} \tag{A9}$$

Equation (A9) is nozzle-type flow (e.g. (Landau & Lifshitz 1975)). The lhs of eq. (A9) contains a familiar critical point at the sonic transition $\Gamma = \Gamma_f$. The positively defined rhs describes the evolution of Lorentz factors due to kinetic pressure effects. In the case of purely radial expansion the magnetic gradient forces are exactly balanced by the hoop stresses, so that magnetic field does not contribute to acceleration. From Eq. (A9) it follows that super-fast-magnetosonic flows accelerate while sub-fast-magnetosonic flows decelerate. It also follows that terminal Lorentz factor of the flow is determined by the condition $\partial_r\Gamma = 0$ which implies that either $p = 0$ or $\beta_\infty = 0$. Condition $\beta_\infty = 0$ can be reached only for subsonic flows with $\mathcal{E} = 0$. Neglecting the $\beta_\infty = 0$ solution, the terminal velocity of magnetized flow is determined by the condition:

$$L = \Gamma_\infty \dot{M} + \frac{\mathcal{E}^2}{\beta_\infty} \tag{A10}$$

For each set of parameters (L, $\dot{M}$ and $\mathcal{E}$) there are generally two solutions of Eq. (A10) for the terminal four-velocity. The only exception is the case of zero magnetization, $\mathcal{E} = 0$, when the terminal (supersonic) Lorentz factor is uniquely determined by $\Gamma_\infty = L/\dot{M}$.

For non-zero magnetization the terminal velocity cannot be determined uniquely from given L, $\dot{M}$ and $\mathcal{E}$. Solutions exist only for $L/\dot{M}$ larger than some critical value $L/\dot{M} = (1 - (\mathcal{E}^2/L)^{2/3})^{-3/2}$, corresponding to $\beta_\infty = (\mathcal{E}^2/L)^{1/3}$. For fixed $\dot{M}$ and $\mathcal{E}$ the minimum energy loss is reached at β_{min}. Assumption $\beta_\infty = \beta_{min}$, then gives

$$\left(1 + (\beta_\infty \Gamma_\infty \sigma_\infty)^{2/3}\right)^{3/2} = \frac{\Gamma_\infty \sigma_\infty}{\beta_\infty^2} \tag{A11}$$

which in the strongly relativistic limit gives Michel solution

$$\Gamma_\infty = \sqrt{\sigma_\infty}. \tag{A12}$$

We can also relate the terminal magnetization σ_∞ to the magnetization at the source - more specifically to magnetization at the sonic point σ_f:

$$\sigma_f = \begin{cases} \frac{\sigma_\infty}{\Gamma_a - 1} & = 3\sigma_\infty \quad \text{if } \sigma_\infty \ll 1 \\ \frac{(4-\Gamma_a)\sigma_\infty}{2} & = \frac{4}{3}\sigma_\infty \quad \text{if } \sigma_\infty \gg 1 \end{cases} \tag{A13}$$

Thus, we always have $\sigma_\infty < \sigma_f$, but they remain of the same order of magnitude: the magnetization of the flow changes only slightly as the flow propagates away from the launching

point to infinity. The reason for constant σ in the supersonic regime is that both in the case $p \gg \rho$ (linear acceleration stage) and $p \ll \rho$ (coasting stage) the plasma and the magnetic field energy densities in the flow change with the same radial dependence ($\sim r^{-4}$ and $\sim r^{-2}$ correspondingly).

For arbitrary flow parameters the evolution equations are integrated numerically (Fig. 3). Given the evolution of the flow and the relation for local σ we can find the evolution of the magnetization parameter (Fig. 3.b).

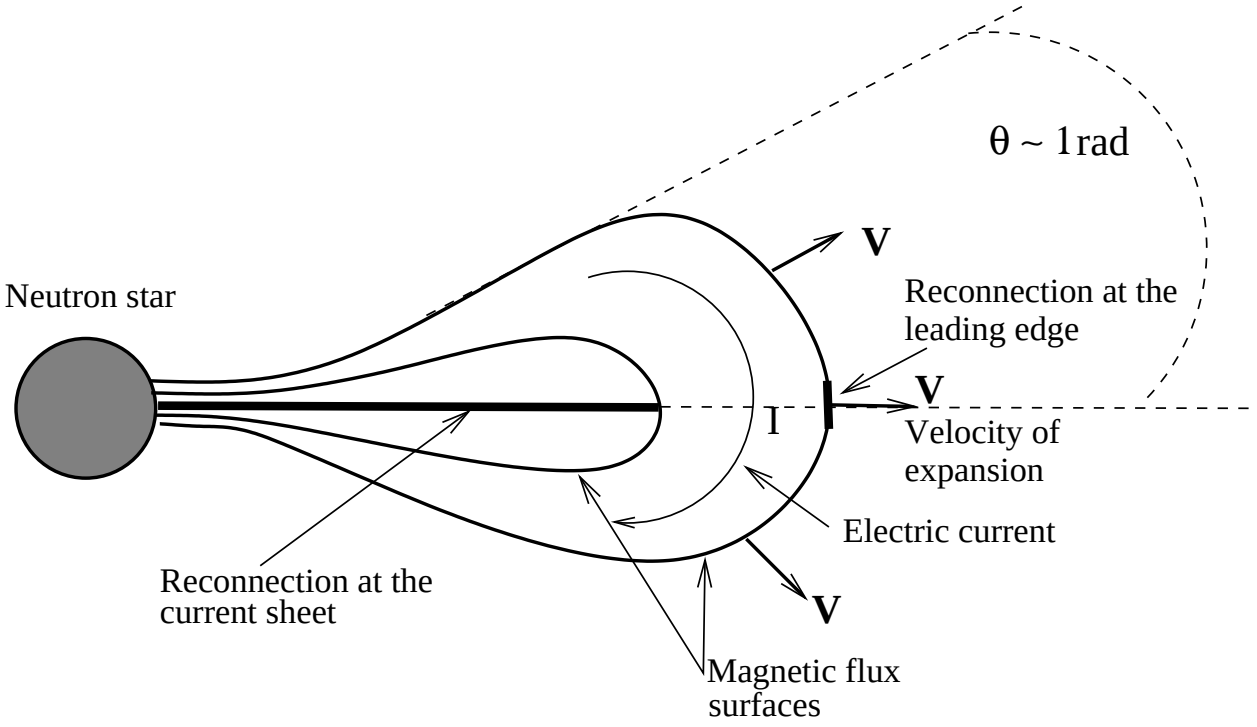

Fig. 1.— Cartoon of an expanding, collimated flux rope. Twisting of footpoints of a flux tube leads to electric current flow along the loop and results in its expansion. Beyond some twist angle dynamic instability leads to formation of dissipative current sheets at the leading edge of the loop, between the footpoints and, possibly in the bulk. Reconnection at the leading edge allows the flux tube to break out of the magnetosphere. Collimating effect of the tied footpoints later lead to broadly collimated outflow.

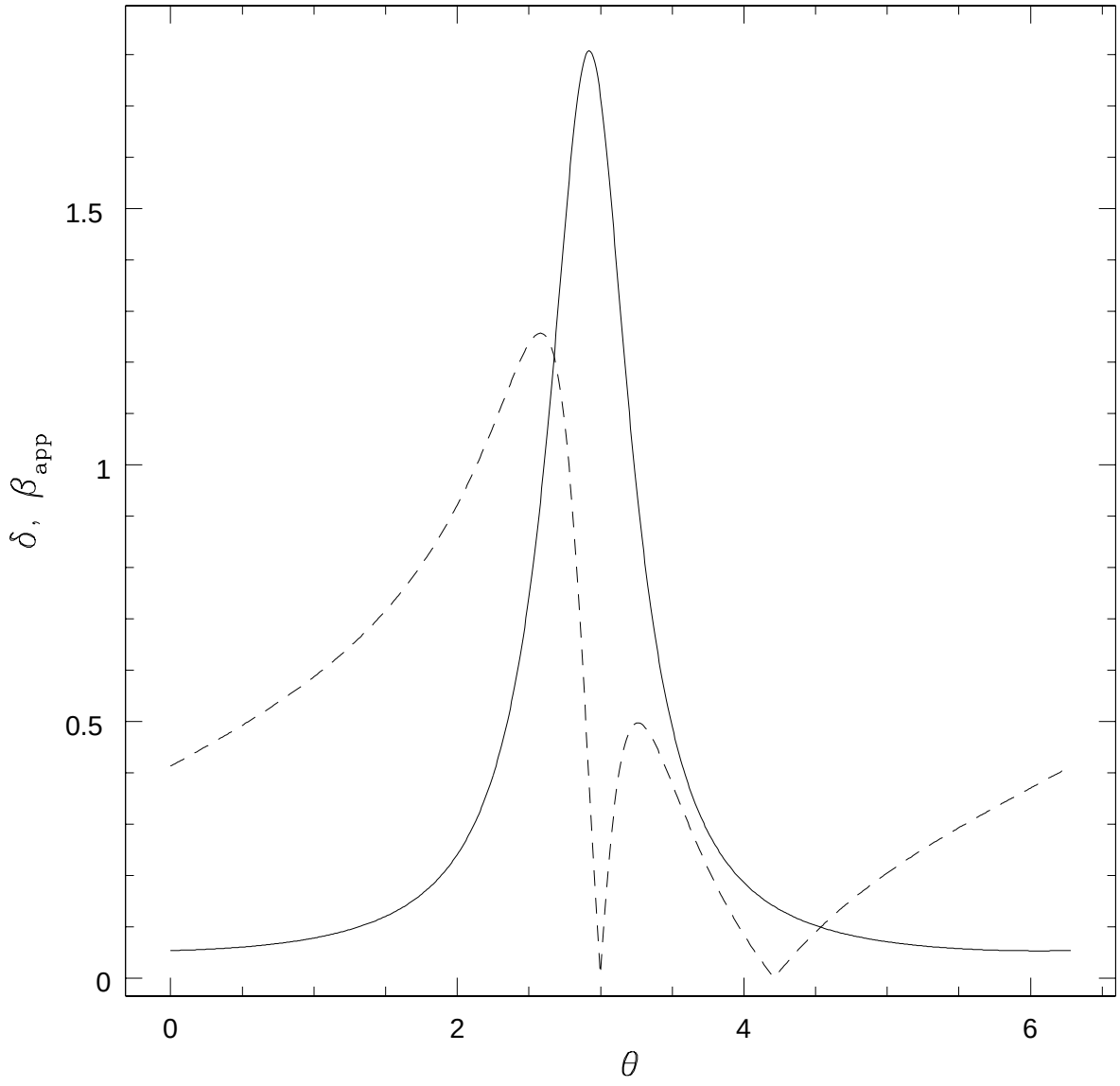

Fig. 2.— Doppler factor $\mathcal{D} = 1/(\Gamma(1 - \beta\cos\theta)$ (solid line) and apparent transverse velocity (dashed line) for a relativistic shock expanding with Lorentz factor $\Gamma = 3$ and moving at $\theta_{ob} = 135^\circ$ with bulk Lorentz factor $\Gamma_{bulk} = 2$ as a function of the angle θ between the explosion direction and the emission point in the rest frame of the explosion for emission points located in the plane containing direction of bulk motion and line of sight.

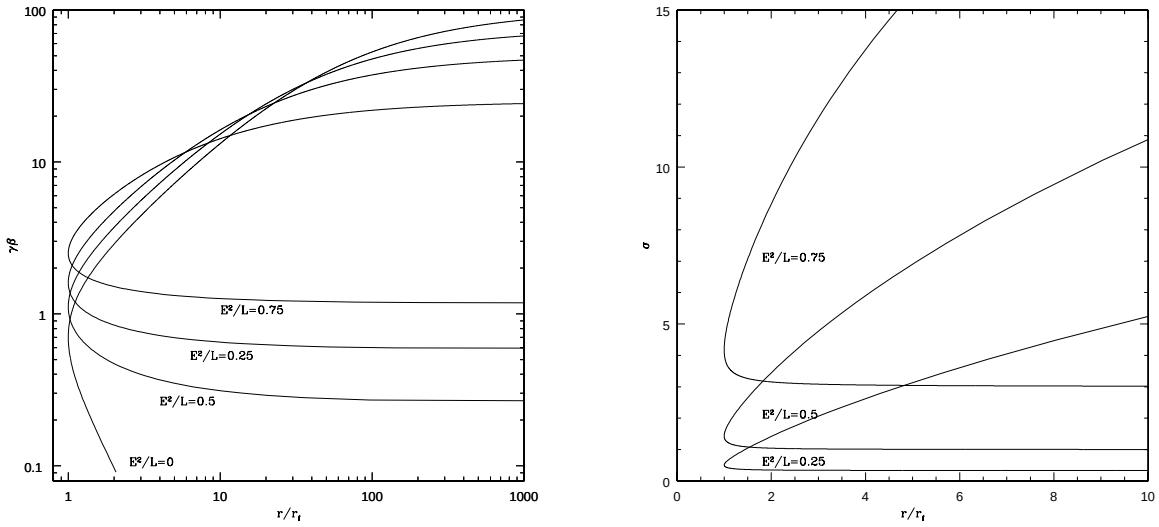

Fig. 3.— Evolution of strongly magnetized and hot flows. (a) Four-velocities of flows are given as functions of r/r_f for $L/\dot{M} = 100$ and different values of the parameter $\frac{\mathcal{E}^2}{L}$. Flows start at $r = r_f$ with $\beta = \beta_f$; supersonic flows first accelerate as $\beta\gamma \sim r$, reaching a terminal value given by the larger root of eq. (A10), while subsonic decelerate initially as $\beta \sim r^{-2}$ reaching asymptotic value given by the smaller root of eq. (A10). (b) Magnetization parameter σ. For supersonic flows (lower branch) the magnetization remains constant, reaching $\sigma_\infty = \left(1 - \frac{\mathcal{E}^2}{L}\right)^{-1}$ as $r \to \infty$. Subsonic flows become strongly magnetized as they expand (upper branch); the magnetization parameter increases $\sigma \sim r^{2/3}$.